A Visible-Light-Driven Molecular Motor Based on Pyrene

Roke, Diederik; Feringa, Ben L.; Wezenberg, Sander J.

Published in:
Helvetica Chimica Acta

DOI:
10.1002/hlca.201800221

DOI: 10.1002/hlca.201800221

COMMUNICATION

HELVETICA chimica acta

A Visible-Light-Driven Molecular Motor Based on Pyrene

Diederik Roke,[a] Ben L. Feringa,*[a] and Sander J. Wezenberg*[a]

[a] Stratingh Institute for Chemistry, University of Groningen, 9747 AG, Groningen, The Netherlands,
e-mail: b.l.feringa@rug.nl; s.j.wezenberg@rug.nl

Dedicated to *François Diederich* on the occasion of his retirement

The aromatic core of an overcrowded alkene-based molecular motor is extended with the goal of inducing isomerization with visible light instead of harmful UV light. In our design, the common naphthalene moiety in the upper half of the motor is changed to pyrene. The photochemical and thermal isomerization processes are studied in detail using DFT calculations as well as NMR and UV/VIS spectroscopy. Our studies confirm that extension of the π-system of the upper half successfully leads to a shift of the excitation wavelength into the visible region, while retaining proper rotary function.

Keywords: isomerization, molecular motors, molecular switches, photochromism, overcrowded alkenes, pyrenes.

Introduction

One of the major challenges in the field of photoresponsive molecular switches and motors is to shift the excitation wavelength from the harmful UV into the visible light region.[1–4] This wavelength shift is necessary to fully exploit the potential for application in biology[5–8] and smart materials.[9–13] Various strategies for the activation of existing photoswitches with visible light have been developed in recent years, mostly by making changes to the photochromic unit in such a way that the absorption extends into the visible light region. Examples are push-pull systems,[14][15] extension of the π-system[16][17] and *ortho*-functionalization (applied to azobenzenes).[18–20] Alternatively, photosensitizers[21][22] or upconverting nanoparticles[23] have been used to operate photoswitches with visible or even near infrared light. Additionally, new types of photoswitches are emerging that allow for switching with visible light.[24–27]

Molecular motors based on overcrowded alkenes are unique photoswitches in the sense that they undergo unidirectional rotary motion around their central double bond axle.[4][28][29] Their rotary cycle is based on two photochemical steps and two thermally activated steps (*Scheme 1,a*). An initial light-induced (*E*/*Z*) isomerization yields a metastable isomer (often referred to as the 'unstable' state) with opposite helicity. Subsequently, a thermal helix inversion (THI) occurs in which the upper half passes the lower half. The second half of the cycle proceeds identically, resulting in 360° rotation. Owing to the unique properties of these molecular motors, they have been applied in diverse fields, such as soft materials,[12][30–32] liquid crystals,[33][34] anion binding,[35][36] and catalysis.[37][38]

Different strategies have been followed to red-shift the excitation wavelength of these motors. For example, by attachment of a tetraphenylporphyrin triplet sensitizer so that irradiation with 530 nm light resulted in triplet-triplet energy transfer from the porphyrin to the molecular motor, driving the rotation.[39] In an alternative approach, a molecular motor was incorporated into a Ru(II)-bipyridine complex.[40] Here, irradiation into the metal-to-ligand charge transfer band with 450 nm light resulted in rotation. Other methods have been applied in which changes to the motor design were made in such a way that it absorbs visible light. However, structural modifications some-

Supporting information for this article is available on the WWW under https://doi.org/10.1002/hlca.201800221

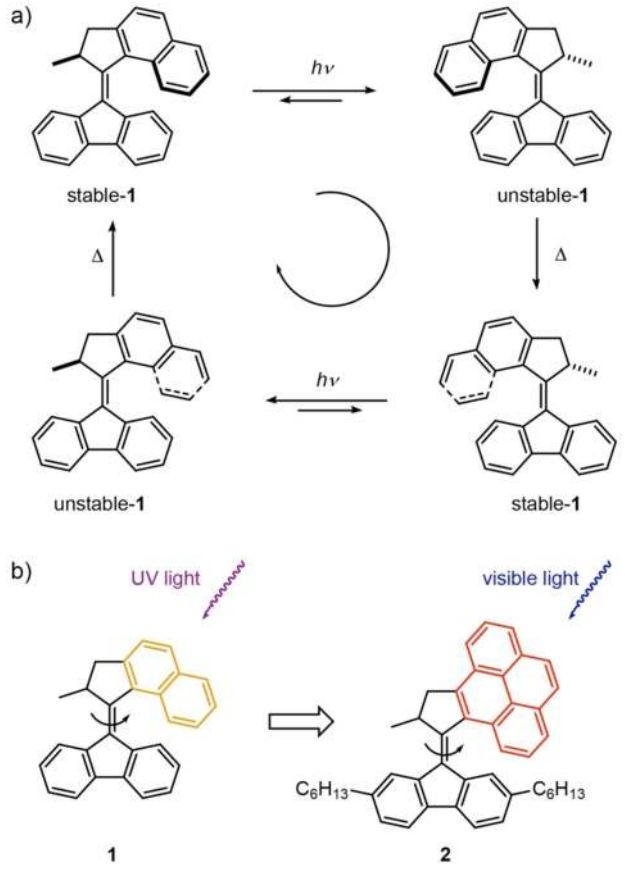

Scheme 1. a) Rotary cycle of a second generation molecular motor. Note that for molecular motors with a symmetric lower half like **1**, the isomer obtained after 180° rotation is identical to the initial isomer. b) Extension of the π system on the upper half of the molecular motor to red-shift its excitation wavelength.

times inhibit the switching and rotary function. The earliest successful example of a molecular motor able to absorb visible light features a push-pull substituent pattern.[41] The motor, bearing a nitro and a dimethylamino substituent, showed photoisomerization with 425 nm light. Recently, our group demonstrated that by extending the π-system of the lower half, the excitation wavelength can also be shifted to the visible region (up to 490 nm).[42] We became interested in applying the same strategy to the upper half and hence, overcrowded alkene **2**, in which the naphthalene moiety in the upper half of parent motor **1** is changed to pyrene, was designed (*Scheme 1,b*). Additionally, alkyl chains are attached to the lower half to improve solubility.

Results and Discussion

To predict whether target compound **2** could function as a visible-light-driven molecular motor, TD-DFT calculations were performed. The structure was optimized and the vertical transitions were calculated using B3LYP/6-31G(d,p), which was shown before to be a reliable method for the prediction of geometries and UV/VIS spectra of overcrowded alkene-based molecular motors.[42][43] To reduce calculation time, methyl instead of hexyl substituents were introduced in the lower half. The first calculated transition at 431 nm has low oscillator strength (0.0038) and therefore most likely will not cause significant absorption. The second transition, being the HOMO–LUMO transition located at 420 nm, has a much higher oscillator strength (0.4818; *Figure 1*). Analysis of the orbitals

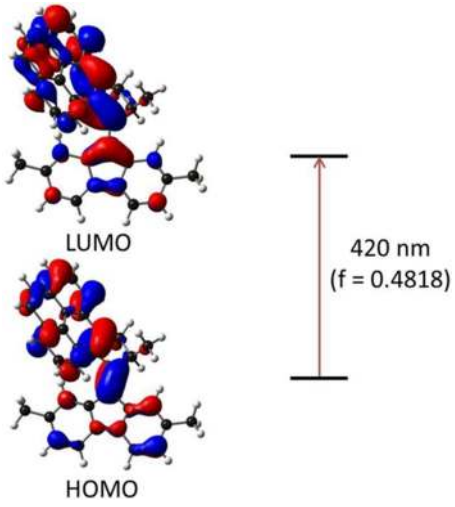

Figure 1. TD-DFT Calculated HOMO–LUMO transition of motor **2**.

involved showed a typical π–π* transition located at the central double bond which is likely to lead to photochemical isomerization.

The same functional and basis set were used to predict the thermal barrier for THI. The ground state and transition state geometries were identified and the geometries were optimized, and subsequently verified with a frequency analysis (see the *Supporting Information* for details). A barrier ($\Delta^{\ddagger}G_{calc}$) of 90.9 kJ mol^{-1} was found, which is slightly higher than the experimentally determined barrier for THI of parent motor **1** ($\Delta^{\ddagger}G_{exp} = 85$ kJ mol^{-1}).[44] As these results indicated that this pyrene-derived overcrowded

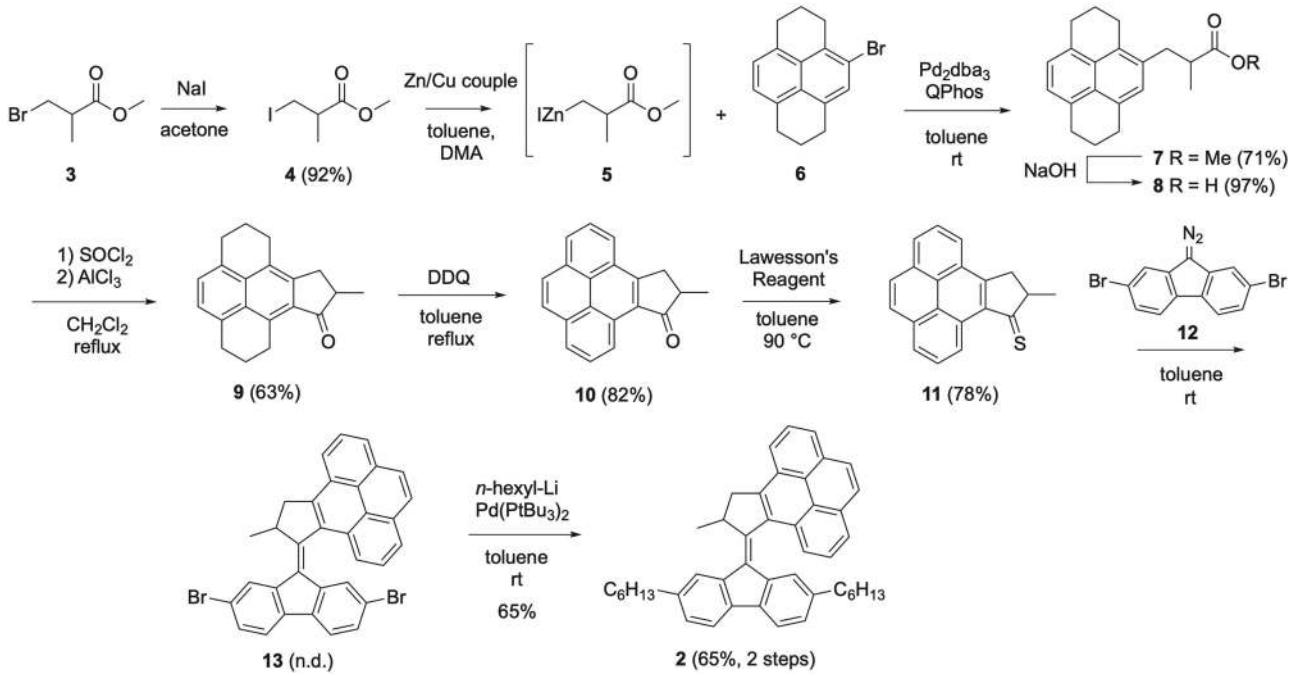

Scheme 2. Synthetic route for pyrene-based molecular motor **2**.

alkene would function as a visible-light-driven motor, we devised a synthetic route towards this compound.

The synthesis of **2** started with a palladium-catalyzed *Negishi* cross-coupling of hexahydropyrene **6** with organozinc reagent **5** (*Scheme 2*). This organozinc reagent was prepared from ester **3**, in which the bromide in **3** was substituted for iodide using a *Finkelstein* reaction to give **4**. Subsequently, compound **4** was transformed into the organozinc reagent **5** by reaction with a zinc-copper couple, after which it was directly submitted to the cross-coupling reaction. The ester in compound **7** was then hydrolyzed and transformed into an acid chloride by using thionyl chloride, which was followed by an $AlCl_3$ mediated intramolecular *Friedel–Crafts* acylation to form ketone **9**. Oxidation of **9** with DDQ afforded pyrene **10**, which was subsequently converted into thioketone **11** and submitted to a *Barton–Kellogg* reaction with diazo compound **12** to provide overcrowded alkene **13**. In the last step, hexyl chains were introduced to the lower half using a double palladium-catalyzed organolithium cross-coupling, which was developed in our group.[45][46] The structure of motor **2** was verified with ^{1}H- and ^{13}C-NMR and the composition was confirmed by HR-MS.

Next, the photochemical and thermal isomerization behavior of motor **2** was investigated using UV/VIS spectroscopy. The UV/VIS spectrum of motor **2** in CH_2Cl_2 showed an absorption maximum in the visible region, at $\lambda = 414$ nm, which is close to the predicted maximum of $\lambda = 420$ nm (*Figure 2*). Upon irradiation with $\lambda_{max} = 455$ nm at 0 °C, a distinct bathochromic shift was observed, which is characteristic for the formation of the unstable state upon photochemical (*E*/*Z*) isomerization. A clear isosbestic point was observed at $\lambda = 425$ nm, indicative of a unimolecular process. Notably, even though pyrene is well-known to be fluorescent,[47][48] no significant fluorescence was

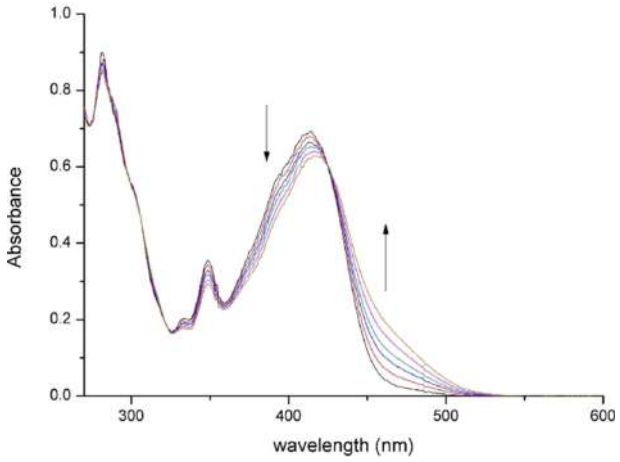

Figure 2. UV/VIS Spectral changes for motor **2** in CH_2Cl_2 ($c = 2.3 \times 10^{-5}$ M) upon irradiation with $\lambda_{max} = 455$ nm.

observed for motor **2**. When the irradiated UV/VIS sample was allowed to warm to room temperature, the original absorption spectrum was obtained, indicating that the unstable state had undergone thermal isomerization to afford the stable state. An *Eyring* analysis was performed to determine the activation parameters for this thermal process. The rate of isomerization was determined at five different temperatures between 0 °C and 20 °C by following the decrease in absorption at $\lambda = 470$ nm (*Figure S2*). The *Gibbs* free energy of activation was found to be ($\Delta^{\ddagger}G$) 88.5 ± 0.1 kJ mol^{-1}, which is in good agreement with the calculated value of 91 kJ mol^{-1} for THI obtained by DFT. As expected, this value is also in the same range as the barrier for THI of parent motor **1** ($\Delta^{\ddagger}G =$ 85 kJ mol^{-1}).

The photochemical and thermal isomerization was also followed by ^{1}H-NMR spectroscopy. Irradiation of a sample of motor **2** in CD_2Cl_2 with $\lambda_{max} = 455$ nm at −25 °C led to the appearance of a new set of signals, indicative of the formation of the unstable state (*Figures 3* and *S5*). The sample was irradiated until no further changes were observed and at this photostationary state (PSS), the ratio of unstable to stable was determined to be 28:72.[1] Irradiation of the same sample with $\lambda_{max} = 395$ nm led to a higher PSS ratio of 90:10 as the unstable state has a lower absorption than the stable state at this wavelength (*Figure 2*).[2] When the sample was allowed to warm to room temperature, the original spectrum was obtained, illustrating that the THI had taken place, while no significant signs of degradation were observed. Combined, these studies show that the pyrene based motor **2** functions as a visible-light-driven molecular motor.

The quantum yield for the photochemical (*E*/*Z*) isomerization ($\Phi_{s\rightarrow u}$) was determined to be 1.4% by comparing the rate of formation of the unstable state to the formation of Fe^{2+} ions from potassium ferrioxalate under identical conditions (see the *Supporting Information* for details). Using the PSS ratio, the quantum yield for the reverse photochemical isomerization ($\Phi_{u\rightarrow s}$) was calculated to be 0.38%. These values are slightly lower than those reported for structurally related molecular motors, but nevertheless are in the same order of magnitude.[49]

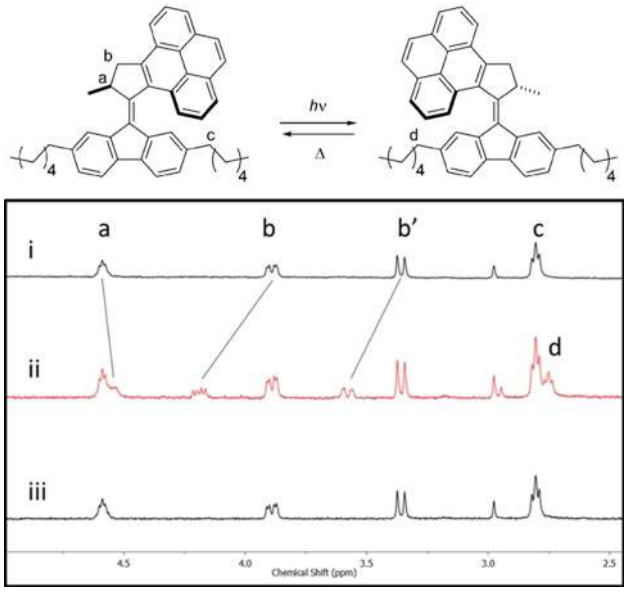

Figure 3. (Top) Photochemical and thermal isomerization of motor **2**. (Bottom) Selected part of the ^{1}H-NMR spectra of motor **2** in CD_2Cl_2 ($c = 1.7 \times 10^{-3}$ M) at −25 °C: i) stable 2, ii) PSS $\lambda_{max} =$ 455 nm, iii) THI, 20 °C.

Conclusions

In summary, aromatic extension of the upper half, from naphthalene to pyrene, is shown to be a viable method to shift the excitation wavelength of a molecular motor into the visible light region ($\lambda_{irr} =$ 455 nm). The photochemical and thermal isomerization processes were first predicted by DFT calculations, which were followed by the successful synthesis of this pyrene-based molecular motor. Combined UV/VIS and ^{1}H-NMR studies revealed that the excitation wavelength is shifted into the visible region, while proper rotary function is retained.

Experimental Section

See *Supporting Information* for general procedures.

[1] A lower PSS ratio is not necessarily a limitation for molecular motors, as the following THI is a forward process in the rotary cycle.

[2] The relation between the PSS ratio and extinction coefficient is given by the following equation: PSS ratio = $\Phi_1\varepsilon_1/\Phi_2\varepsilon_2$.

Methyl 3-Iodo-2-methylpropanoate (**4**). NaI (375 mg, 2.5 mmol) was added to a solution of methyl-(2*R*)-3-bromo-2-methylpropanoate (0.25 ml, 2.0 mmol) in acetone (1.5 ml). The mixture was stirred at reflux for 2 h, after which water was added (5 ml). The mixture was extracted three times with Et_2O and the combined organic layers were dried over $MgSO_4$. The volatiles were carefully removed *in vacuo* (> 500 mbar) and the residue was filtered over a plug of silica (Et_2O). The ether was evaporated *in vacuo* to yield compound **4** (417 mg, 92%) as a red oil. ^{1}H-NMR (400 MHz, $CDCl_3$): 3.73 (*s*, 3 H); 3.38 (*dd*, *J* = 9.8, 6.6, 1 H); 3.26 (*dd*, *J* = 9.8, 6.2, 1 H); 2.80 (*sext.*, *J* = 6.8, 1 H); 1.28 (*d*, *J* = 7.0, 3 H). Spectroscopic data are in agreement with those reported in the literature.[50]

Methyl 3-(1,2,3,6,7,8-Hexahydropyren-4-yl)-2-methylpropanoate (**7**). A solution of iodide **4** (240 mg, 1.05 mmol) in dry toluene/DMA (15 : 1, 4.3 ml) was added to Zn–Cu couple (126 mg) under a N_2 atmosphere. The mixture was stirred at 60 °C for 4 h after which it was cooled down to room temperature. Then, 4-bromo-1,2,3,6,7,8-hexahydropyrene (271 mg, 0.945 mmol), Pd_2dba_3 (10.8 mg, 0.0118 mmol) and QPhos (16.8 mg, 0.0236 mmol) were added as solids, and the mixture was stirred at room temperature overnight. The suspension was filtered over *Celite* (flushed with CH_2Cl_2) and the volatiles were removed *in vacuo*. The residue was purified by column chromatography (SiO_2, pentane/AcOEt 30 : 1) to yield **7** (208 mg, 71%) as a yellow solid. ^{1}H-NMR (400 MHz, $CDCl_3$): 7.16 (*d*, *J* = 7.1, 1 H); 7.13 (*d*, *J* = 7.1, 1 H); 7.06 (*s*, 1 H); 3.70 (*s*, 3 H); 3.29–3.18 (*m*, 1 H); 3.15–3.02 (*m*, 8 H); 2.91–2.79 (*m*, 2 H); 2.13–2.03 (*m*, 4 H); 1.23 (*d*, *J* = 6.3, 3 H). ^{13}C-NMR (100 MHz, $CDCl_3$): 176.9; 134.0; 134.0; 133.7; 132.2; 131.3; 130.4; 129.1; 126.4; 123.7; 123.0; 51.6; 40.5; 36.9; 31.5; 31.5; 31.4; 27.7; 23.3; 23.1; 16.8. HR-ESI-MS (pos.): 309.1848 ($C_{21}H_{25}O_2^+$, $[M+H]^+$; calc. 309.1849).

3-(1,2,3,6,7,8-Hexahydropyren-4-yl)-2-methylpropanoic Acid (**8**). Methyl ester **7** (364 mg, 1.18 mmol) was dissolved in 25 ml THF and 25 ml aqueous 0.1 M NaOH. The mixture was stirred overnight at room temperature after which it was acidified with 2 M aq. HCl. The mixture was extracted with CH_2Cl_2, and the combined organic layers were dried over $MgSO_4$. The volatiles were removed *in vacuo* to yield **8** (340 mg, 97%) as a colorless oil. ^{1}H-NMR (400 MHz, $CDCl_3$): 7.14 (*d*, *J* = 7.1, 1 H); 7.11 (*d*, *J* = 7.1, 1 H); 7.05 (*s*, 1 H); 3.33–3.20 (*m*, 1 H); 3.07 (*q*, *J* = 5.4, 8 H); 2.94–2.75 (*m*, 2 H); 2.12–2.00 (*m*, 4 H); 1.22 (*d*, *J* = 6.5, 3 H). ^{13}C-NMR (100 MHz, $CDCl_3$): 182.9; 134.2; 134.2; 133.9; 132.0; 131.5; 130.5; 129.3; 126.5; 123.9; 123.2; 40.6; 36.6; 31.6; 31.5; 27.8; 23.4; 23.2; 16.6. HR-ESI-MS (pos.): 295.1691 ($C_{20}H_{23}O_2^+$, $[M+H]^+$; calc. 295.1693).

10-Methyl-1,2,3,6,7,8,10,11-octahydro-9*H*-cyclopenta[*e*]pyren-9-one (**9**). Acid **8** (340 mg, 1.15 mmol) was dissolved in dry CH_2Cl_2 (25 ml) under N_2 atmosphere. Thionyl chloride (0.20 ml, 2.74 mmol) was added, and the mixture was stirred at reflux for 4 h. The volatiles were removed *in vacuo* and the residue was again dissolved in dry CH_2Cl_2 (25 ml) under N_2 atmosphere. $AlCl_3$ (231 mg, 1.73 mmol) was added in portions at 0 °C, and the mixture was stirred at reflux for 3 h. The mixture was left to stir at room temperature overnight after which water was carefully added. The layers were separated, and the aqueous layer was extracted with CH_2Cl_2. The combined organic layers were washed with water and dried over $MgSO_4$. The volatiles were removed *in vacuo* and the residue was purified using column chromatography (SiO_2, pentane/AcOEt 20 : 1) to yield compound **9** (200 mg, 63%) as a colorless oil. ^{1}H-NMR (400 MHz, $CDCl_3$): 7.23 (*d*, *J* = 7.0, 1 H); 7.11 (*d*, *J* = 7.0, 1 H); 3.62 (*t*, *J* = 6.3, 2 H); 3.39 (*dd*, *J* = 16.7, 8.4, 1 H); 3.07 (*t*, *J* = 6.2, 4 H); 3.03–2.95 (*m*, 2 H); 2.83–2.71 (*m*, 1 H); 2.67 (*dd*, *J* = 16.7, 4.9, 1 H); 2.14–1.99 (*m*, 4 H); 1.36 (*d*, *J* = 7.3, 3 H). ^{13}C-NMR (100 MHz, $CDCl_3$): 211.6; 142.6; 137.4; 137.2; 133.7; 133.0; 129.6; 129.5; 128.1; 126.4; 123.5; 43.0; 32.9; 31.2; 31.2; 27.0; 26.6; 22.9; 22.6; 16.9. HR-ESI-MS (pos.): 277.1590 ($C_{20}H_{21}O^+$, $[M+H]^+$; calc. 277.1587).

(10*S*)-10-Methyl-10,11-dihydro-9*H*-cyclopenta[*e*]pyren-9-one (**10**). Ketone **9** (280 mg, 1.01 mmol) was dissolved in dry toluene (50 ml) under N_2 atmosphere and DDQ (722 mg, 3.18 mmol) was added. The mixture was heated at reflux for 2 h and left to cool down to room temperature. The suspension was filtered over *Celite* (flushed with CH_2Cl_2) and the volatiles were removed *in vacuo*. The residue was purified by column chromatography (SiO_2, CH_2Cl_2) to yield **10** (225 mg, 82%) as a yellow oil. ^{1}H-NMR (400 MHz, $CDCl_3$): 9.50 (*d*, *J* = 7.7, 1 H); 8.37–8.31 (*m*, 2 H); 8.22 (*d*, *J* = 7.5, 1 H); 8.14–8.03 (*m*, 4 H); 3.86 (*dd*, *J* = 17.6, 7.3, 1 H); 3.16 (*dd*, *J* = 17.6, 3.1, 1 H); 3.02 (*quint. d*, *J* = 7.4, 3.0, 1 H); 1.51 (*d*, *J* = 7.5, 3 H). ^{13}C-NMR (100 MHz, $CDCl_3$): 212.8; 160.3; 134.0; 133.4; 132.1; 131.0; 130.7; 130.5; 129.6; 129.2; 128.8; 128.7; 128.4; 128.4; 126.8; 125.0; 124.7; 124.7; 44.5; 36.0; 19.5. HR-ESI-MS (pos.): 271.1109 ($C_{20}H_{15}O^+$, $[M+H]^+$; calc. 271.1117).

9-(2,7-Dibromo-9*H*-fluoren-9-ylidene)-10-methyl-10,11-dihydro-9*H*-cyclopenta[*e*]pyrene (**13**). Ketone **10** (196 mg, 0.725 mmol) and *Lawesson* reagent (441 mg, 1.09 mmol) were dissolved in dry toluene (5 ml) under N_2 atmosphere. The resulting suspension was heated to 95 °C, and the conversion was followed by TLC. After 2.5 h, the mixture was allowed to cool down to room temperature and directly purified using column chromatography (SiO_2, pentane/CH_2Cl_2 4:1→2:1) to yield the corresponding thioketone (161 mg, 78%), which was used directly in the following reaction.

Thioketone **11** (160 mg, 0.559 mmol) and diazo compound **12** (294 mg, 0.839 mmol) were dissolved in dry toluene under a N_2 atmosphere. The mixture was stirred overnight at room temperature and subsequently for 24 h at 70 °C, after which full conversion of the thioketone was observed. HMPT (0.17 ml, 0.923 mmol) was added, and the mixture was stirred for 4 h at 70 °C. Water was added, and the layers were separated. The aqueous layer was extracted twice with CH_2Cl_2, and the combined organic layers were washed with brine and dried over $MgSO_4$. The volatiles were removed *in vacuo*, and the resulting solids were washed with AcOEt. The crude product was used in the following reaction without further purification.

9-(2,7-Dihexyl-9*H*-fluoren-9-ylidene)-10-methyl-10,11-dihydro-9*H*-cyclopenta[*e*]pyrene (**2**). Compound **13** (50 mg, 0.0868 mmol) and $Pd[P(tBu)_3]_2$ (4.4 mg, 0.00868 mmol) were loaded in a dry *Schlenk* flask under N_2 atmosphere. Dry toluene (4 ml) was added) and the mixture was purged with O_2 and stirred overnight. In a separate dry *Schlenk* flask, hexyllithium (2.2 M, 0.5 ml) was diluted with toluene (4.5 ml) to reach a final concentration of 0.22 M. Diluted hexyllithium (0.8 ml) was added over 1 h *via* a syringe pump to the mixture of compound **13** and catalyst at room temperature and stirred for an additional 30 min. The mixture was treated with MeOH (0.1 ml) and the volatiles were removed *in vacuo*. The residue was purified by column chromatography to yield compound **2** (33 mg, 65%) as a dark yellow solid. ^{1}H-NMR (400 MHz, $CDCl_3$): 8.30 (*d*, *J* = 7.7, 2 H); 8.21 (*d*, *J* = 7.9, 1 H); 8.18–8.07 (*m*, 4 H); 7.88 (*s*, 1 H); 7.80 (*t*, *J* = 7.7, 1 H); 7.72 (*d*, *J* = 7.7, 1 H); 7.60 (*d*, *J* = 7.6, 1 H); 7.22 (*dd*, *J* = 7.8, 1.3, 1 H); 6.96 (*dd*, *J* = 7.6, 1.5, 1 H); 6.39 (*s*, 1 H); 4.57 (*quint.*, *J* = 6.5, 1 H); 3.87 (*dd*, *J* = 15.2, 5.6, 1 H); 3.31 (*d*, *J* = 15.2, 1 H); 2.79 (*t*, *J* = 7.6, 2 H); 2.04–1.86 (*m*, 2 H); 1.77 (*quint.*, *J* = 7.5, 2 H); 1.54 (*d*, *J* = 6.6, 3 H); 1.50–1.31 (*m*, 6 H); 1.10 (*quint.*, *J* = 6.9, 2 H); 1.05–0.68 (*m*, 12 H). ^{13}C-NMR (100 MHz, $CDCl_3$): 153.0; 148.8; 143.9; 142.9; 142.7; 140.8; 140.1; 140.0; 138.8; 134.3; 134.1; 133.6; 132.0; 130.8; 130.0; 130.0; 129.9; 129.5; 129.4; 128.8; 128.7; 128.6; 128.5; 127.8; 127.6; 127.0; 126.9; 125.0; 121.8; 120.9; 47.6; 43.0; 39.2; 38.4; 34.5; 34.5; 34.2; 33.4; 31.7; 31.5; 25.4; 25.1; 22.3; 16.8; 16.8. HR-ESI-MS (pos.): 587.3660 ($C_{45}H_{47}^+$, $[M+H]^+$; calc. 587.3678).

Acknowledgements

This work was supported by NanoNed, The Netherlands Organization for Scientific Research (Top grant to *B. L. F.* and Veni Grant 722.014.006 to *S. J. W.*), the Royal Netherlands Academy of Arts and Sciences, the Ministry of Education, Culture and Science (Gravitation programme 024.001.035), and the European Research Council (Advanced Investigator Grant 694345 to *B. L. F.*). We would like to thank the Center for Information Technology of the University of Groningen for their support and for providing access to the Peregrine high performance computing cluster.

Author Contribution Statement

B. L. F. and *S. J. W.* conceived the project, *D. R.* performed the calculations, synthesis and spectroscopic studies, and *B. L. F.* and *S. J. W.* supervised the project. *D. R.*, *B. L. F.* and *S. J. W.* wrote the manuscript.

References

[1] B. L. Feringa, W. R. Browne, 'Molecular Switches', Vol. 1, 2nd Edn., Wiley-VCH Verlag GmbH & Co. KGaA, Weinheim, Germany, 2011.
[2] D. Bléger, S. Hecht, 'Visible-Light-Activated Molecular Switches', *Angew. Chem. Int. Ed.* **2015**, *54*, 11338–11349.
[3] S. Kassem, T. van Leeuwen, A. S. Lubbe, M. R. Wilson, B. L. Feringa, D. A. Leigh, 'Artificial molecular motors', *Chem. Soc. Rev.* **2017**, *46*, 2592–2621.
[4] D. Roke, S. J. Wezenberg, B. L. Feringa, 'Molecular rotary motors: Unidirectional motion around double bonds.', *Proc. Natl. Acad. Sci. USA* **2018**, *115*, 9423–9431.
[5] M. M. Lerch, M. J. Hansen, G. M. van Dam, W. Szymanski, B. L. Feringa, 'Emerging Targets in Photopharmacology', *Angew. Chem. Int. Ed.* **2016**, *55*, 10978–10999.
[6] J. Broichhagen, J. A. Frank, D. Trauner, 'A Roadmap to Success in Photopharmacology', *Acc. Chem. Res.* **2015**, *48*, 1947–1960.
[7] M. Dong, A. Babalhavaeji, S. Samanta, A. A. Beharry, G. A. Woolley, 'Red-Shifting Azobenzene Photoswitches for in Vivo Use', *Acc. Chem. Res.* **2015**, *48*, 2662–2670.

[8] W. A. Velema, W. Szymanski, B. L. Feringa, 'Photopharmacology: Beyond Proof of Principle', *J. Am. Chem. Soc.* **2014**, *136*, 2178–2191.
[9] S. Saha, J. F. Stoddart, 'Photo-driven molecular devices', *Chem. Soc. Rev.* **2007**, *36*, 77–92.
[10] M.-M. Russew, S. Hecht, 'Photoswitches: From Molecules to Materials', *Adv. Mater.* **2010**, *22*, 3348–3360.
[11] D.-H. Qu, Q.-C. Wang, Q.-W. Zhang, X. Ma, H. Tian, 'Photoresponsive Host–Guest Functional Systems', *Chem. Rev.* **2015**, *115*, 7543–7588.
[12] Q. Li, G. Fuks, E. Moulin, M. Maaloum, M. Rawiso, I. Kulic, J. T. Foy, N. Giuseppone, 'Macroscopic contraction of a gel induced by the integrated motion of light-driven molecular motors', *Nat. Nanotechnol.* **2015**, *10*, 161–165.
[13] T. van Leeuwen, A. S. Lubbe, P. Štacko, S. J. Wezenberg, B. L. Feringa, 'Dynamic control of function by light-driven molecular motors', *Nat. Rev. Chem.* **2017**, *1*, 0096.
[14] A. Mourot, M. A. Kienzler, M. R. Banghart, T. Fehrentz, F. M. E. Huber, M. Stein, R. H. Kramer, D. Trauner, 'Tuning Photochromic Ion Channel Blockers', *ACS Chem. Neurosci.* **2011**, *2*, 536–543.
[15] J. Garcia-Amorós, A. Bučinskas, M. Reig, S. Nonell, D. Velasco, 'Fastest molecular photochromic switches based on nanosecond isomerizing benzothiazolium azophenolic salts', *J. Mater. Chem. C* **2014**, *2*, 474–480.
[16] G. M. Tsivgoulis, J.-M. Lehn, 'Multiplexing optical systems: Multicolor-bifluorescent-biredox photochromic mixtures', *Adv. Mater.* **1997**, *9*, 627–630.
[17] T. Fukaminato, T. Hirose, T. Doi, M. Hazama, K. Matsuda, M. Irie, 'Molecular Design Strategy toward Diarylethenes That Photoswitch with Visible Light', *J. Am. Chem. Soc.* **2014**, *136*, 17145–17154.
[18] A. A. Beharry, O. Sadovski, G. A. Woolley, 'Azobenzene Photoswitching without Ultraviolet Light', *J. Am. Chem. Soc.* **2011**, *133*, 19684–19687.
[19] D. Bléger, J. Schwarz, A. M. Brouwer, S. Hecht, '*o*-Fluoroazobenzenes as Readily Synthesized Photoswitches Offering Nearly Quantitative Two-Way Isomerization with Visible Light', *J. Am. Chem. Soc.* **2012**, *134*, 20597–20600.
[20] M. J. Hansen, M. M. Lerch, W. Szymanski, B. L. Feringa, 'Direct and Versatile Synthesis of Red-Shifted Azobenzenes', *Angew. Chem. Int. Ed.* **2016**, *55*, 13514–13518.
[21] R. T. F. Jukes, V. Adamo, F. Hartl, P. Belser, L. De Cola, 'Photochromic Dithienylethene Derivatives Containing Ru (II) or Os(II) Metal Units. Sensitized Photocyclization from a Triplet State', *Inorg. Chem.* **2004**, *43*, 2779–2792.
[22] C.-C. Ko, V. W.-W. Yam, 'Coordination Compounds with Photochromic Ligands: Ready Tunability and Visible Light-Sensitized Photochromism', *Acc. Chem. Res.* **2018**, *51*, 149–159.
[23] C.-J. Carling, J.-C. Boyer, N. R. Branda, 'Remote-Control Photoswitching Using NIR Light', *J. Am. Chem. Soc.* **2009**, *131*, 10838–10839.
[24] C.-Y. Huang, A. Bonasera, L. Hristov, Y. Garmshausen, B. M. Schmidt, D. Jacquemin, S. Hecht, '*N*,*N*'-Disubstituted Indigos as Readily Available Red-Light Photoswitches with Tunable Thermal Half-Lives', *J. Am. Chem. Soc.* **2017**, *139*, 15205–15211.
[25] C. Petermayer, S. Thumser, F. Kink, P. Mayer, H. Dube, 'Hemiindigo: Highly Bistable Photoswitching at the Biooptical Window', *J. Am. Chem. Soc.* **2017**, *139*, 15060–15067.
[26] S. Helmy, F. A. Leibfarth, S. Oh, J. E. Poelma, C. J. Hawker, J. Read de Alaniz, 'Photoswitching Using Visible Light: A New Class of Organic Photochromic Molecules', *J. Am. Chem. Soc.* **2014**, *136*, 8169–8172.
[27] M. M. Lerch, W. Szymański, B. L. Feringa, 'The (photo) chemistry of Stenhouse photoswitches: guiding principles and system design', *Chem. Soc. Rev.* **2018**, *47*, 1910–1937.
[28] N. Koumura, R. W. J. Zijlstra, R. A. van Delden, N. Harada, B. L. Feringa, 'Light-driven monodirectional molecular rotor', *Nature* **1999**, *401*, 152–155.
[29] N. Koumura, E. M. Geertsema, M. B. Van Gelder, A. Meetsma, B. L. Feringa, 'Second Generation Light-Driven Molecular Motors. Unidirectional Rotation Controlled by a Single Stereogenic Center with Near-Perfect Photoequilibria and Acceleration of the Speed of Rotation by Structural Modification', *J. Am. Chem. Soc.* **2002**, *124*, 5037–5051.
[30] J. Chen, F. K.-C. Leung, M. C. A. Stuart, T. Kajitani, T. Fukushima, E. van der Giessen, B. L. Feringa, 'Artificial muscle-like function from hierarchical supramolecular assembly of photoresponsive molecular motors', *Nat. Chem.* **2018**, *10*, 132–138.
[31] D. J. van Dijken, J. Chen, M. C. A. Stuart, L. Hou, B. L. Feringa, 'Amphiphilic Molecular Motors for Responsive Aggregation in Water', *J. Am. Chem. Soc.* **2016**, *138*, 660–669.
[32] J. T. Foy, Q. Li, A. Goujon, J.-R. Colard-Itté, G. Fuks, E. Moulin, O. Schiffmann, D. Dattler, D. P. Funeriu, N. Giuseppone, 'Dual-light control of nanomachines that integrate motor and modulator subunits', *Nat. Nanotechnol.* **2017**, *12*, 540–545.
[33] R. Eelkema, M. M. Pollard, J. Vicario, N. Katsonis, B. S. Ramon, C. W. M. Bastiaansen, D. J. Broer, B. L. Feringa, 'Molecular machines: Nanomotor rotates microscale objects', *Nature* **2006**, *440*, 163–163.
[34] T. Orlova, F. Lancia, C. Loussert, S. Iamsaard, N. Katsonis, E. Brasselet, 'Revolving supramolecular chiral structures powered by light in nanomotor-doped liquid crystals', *Nat. Nanotechnol.* **2018**, *13*, 304–308.
[35] S. J. Wezenberg, M. Vlatković, J. C. M. Kistemaker, B. L. Feringa, 'Multi-State Regulation of the Dihydrogen Phosphate Binding Affinity to a Light- and Heat-Responsive Bis-Urea Receptor', *J. Am. Chem. Soc.* **2014**, *136*, 16784–16787.
[36] M. Vlatković, B. L. Feringa, S. J. Wezenberg, 'Dynamic Inversion of Stereoselective Phosphate Binding to a Bisurea Receptor Controlled by Light and Heat', *Angew. Chem. Int. Ed.* **2016**, *55*, 1001–1004.
[37] J. Wang, B. L. Feringa, 'Dynamic Control of Chiral Space in a Catalytic Asymmetric Reaction Using a Molecular Motor', *Science* **2011**, *331*, 1429–1432.
[38] D. Zhao, T. M. Neubauer, B. L. Feringa, 'Dynamic control of chirality in phosphine ligands for enantioselective catalysis', *Nat. Commun.* **2015**, *6*, 6652.
[39] A. Cnossen, L. Hou, M. M. Pollard, P. V. Wesenhagen, W. R. Browne, B. L. Feringa, 'Driving Unidirectional Molecular Rotary Motors with Visible Light by Intra- And Intermolecular Energy Transfer from Palladium Porphyrin', *J. Am. Chem. Soc.* **2012**, *134*, 17613–17619.
[40] S. J. Wezenberg, K. Y. Chen, B. L. Feringa, 'Visible-Light-Driven Photoisomerization and Increased Rotation Speed

of a Molecular Motor Acting as a Ligand in a Ruthenium(II) Complex', *Angew. Chem. Int. Ed.* **2015**, *54*, 11457–11461.

[41] R. A. van Delden, N. Koumura, A. Schoevaars, A. Meetsma, B. L. Feringa, 'A donor–acceptor substituted molecular motor: unidirectional rotation driven by visible light', *Org. Biomol. Chem.* **2003**, *1*, 33–35.

[42] T. van Leeuwen, J. Pol, D. Roke, S. J. Wezenberg, B. L. Feringa, 'Visible-Light Excitation of a Molecular Motor with an Extended Aromatic Core', *Org. Lett.* **2017**, *19*, 1402–1405.

[43] A. Cnossen, J. C. M. Kistemaker, T. Kojima, B. L. Feringa, 'Structural Dynamics of Overcrowded Alkene-Based Molecular Motors during Thermal Isomerization', *J. Org. Chem.* **2014**, *79*, 927–935.

[44] J. Vicario, A. Meetsma, B. L. Feringa, 'Controlling the speed of rotation in molecular motors. Dramatic acceleration of the rotary motion by structural modification', *Chem. Commun.* **2005**, 5910–5912.

[45] M. Giannerini, M. Fañanás-Mastral, B. L. Feringa, 'Direct catalytic cross-coupling of organolithium compounds', *Nat. Chem.* **2013**, *5*, 667–672.

[46] D. Heijnen, F. Tosi, C. Vila, M. C. A. Stuart, P. H. Elsinga, W. Szymanski, B. L. Feringa, 'Oxygen Activated, Palladium Nanoparticle Catalyzed, Ultrafast Cross-Coupling of Organolithium Reagents', *Angew. Chem. Int. Ed.* **2017**, *56*, 3354–3359.

[47] K. Kalyanasundaram, J. K. Thomas, 'Environmental effects on vibronic band intensities in pyrene monomer fluorescence and their application in studies of micellar systems', *J. Am. Chem. Soc.* **1977**, *99*, 2039–2044.

[48] B. Valeur, 'Molecular Fluorescence', Wiley-VCH Verlag GmbH, Weinheim, 2001.

[49] J. Conyard, A. Cnossen, W. R. Browne, B. L. Feringa, S. R. Meech, 'Chemically Optimizing Operational Efficiency of Molecular Rotary Motors', *J. Am. Chem. Soc.* **2014**, *136*, 9692–9700.

[50] A. L. Featherston, S. J. Miller, 'Synthesis and evaluation of phenylalanine-derived trifluoromethyl ketones for peptide-based oxidation catalysis', *Bioorg. Med. Chem.* **2016**, *24*, 4871–4874.

Received November 23, 2018
Accepted January 3, 2019